H ∞ Observer for Damper Force in a Semi-Active Suspension

Alfonso Estrada Vela, Diana Hernández Alcantara, Ruben Morales Menendez, Olivier Sename, Luc Dugard

H_∞ Observer for Damper Force in a Semi-Active Suspension ⋆

Alfonso Estrada Vela, Diana Hernández Alcantara *
Ruben Morales Menendez * **Oliver Sename and Luc Dugard** **

* *Tecnológico de Monterrey, School of Engineering and Sciences Monterrey NL, México, {A01175323, dianahalc, rmm}@itesm.mx*
** *Gipsa-Lab INPG Grenoble, France, {olivier.sename, luc.dugard}@gipsa-lab.grenoble-inp.fr*

Abstract: An H_∞ observer for the *Semi-Active (SA)* force of an *Electro-Rheological (ER)* damper in a *Quarter of Vehicle (QoV)* model is proposed. This robust observer is designed in the H_∞ framework to minimize the effect of the unknown road disturbance on the force estimation and includes the damper nonlinearities and its dynamic behavior. Simulation and experimental rig tests results using a 1/5 scale car using easily accessible measurements for the observer, such as acceleration sensors, which are relatively cheap and easy to implement in a real environment. The estimated damper force could be used in a state feedback control strategy to improve comfort and road holding performance of a vehicle with a reduced number of sensors.

Keywords: H_∞-observer, State Estimation, Semi-active suspension, Linear Matrix Inequalities

1. INTRODUCTION

The vehicle suspension system provides the ride comfort and handling characteristics during different driving situations. A passive suspension design implies a trade-off in the vertical vehicle dynamics behavior and *SA* suspensions can be used to overcome this compromise. Its main characteristic is the use of a shock absorbers with a variable damping coefficient, modified by an external control input. They bring very important advantages over passive or active systems since they can approximate the performance of an active suspension. They are preferred in the automotive industry since they work without actuators, low energy consumption, are less bulky and at a lower cost.

To achieve the wanted performance, *SA* suspensions depend upon a control system. Force controllers are frequently designed, these controllers compute the demanded damping force to fulfill the performance specifications. Nonetheless, the damping force computation is not straightforward, mainly due to non-linear characteristics of *SA* dampers and since the actual damper manipulation is either voltage or current, there is a need to transform from the desired damping force to the needed manipulation.

A *FCS* of a *SA* damper is proposed in Besinger et al. (1995), a force feedback control strategy, which adjusts the damping rate according to the measured and desired damping forces. A similar research, where a model of an *ER* damper under proportional feedback control is derived in Sims et al. (1997), the generated force is measured and fed back via a sensor with a certain gain and then compared with a reference force. Batterbee and Sims (2007) validated the force feedback linearization algorithm for an *ER* damper in a vehicle suspension under real road disturbance conditions, using a force sensor to measure the damper force and an *LVDT* sensor to measure the suspension deflection in an experimental facility.

In Vivas-Lopez et al. (2015) a *FCS*, based on feedback linearization, was proposed to improve a *LPV* control system. It takes the *ER* damper non-linear dynamic behavior into account. The *FCS* adjusts the manipulation to reach the reference force, regardless the uncontrolled variables in the force control loop, however, this scheme requires the force measurement. A methodology to estimate the state variables in a full-car vertical model with the design of an H_∞ observer for suspension control applications was proposed in Dugard et al. (2012), allowing to minimize the unknown ground disturbances effects on the estimated state variables. Experimental results in a real car validates the observer.

Eroglu and Sims (2014) established a control algorithm in a *MR* damper. The aim is to perform optimal *force-feedback* linearization of the *MR* damper using an observation of the feedback force with an accelerometer rather than the measured value. However, this work considers a simplified *Single Degree Of Freedom (SDOF)* model, and considers the disturbance as a known input, which makes unfeasible for vehicle suspension applications. A robust H_∞ observer to estimate the force in an *ER* damper is proposed . The observer considers the non linear characteristics of a real *ER* damper taking its dynamical response into account, it achieves an accurate and reliable force estimation in an *ER* damper with a reduced number of sensors.

This paper is organized as follows. Section 2 describes the suspension system model. Section 3 presents in detail the observer design approach. Section 4 discusses the simulation and experimental results. Finally, section 5

⋆ Authors thank *Tecnológico de Monterrey* and *CONACyT* for their partial support.

concludes this research. Table 1 describes the variables used in this paper.

2. SUSPENSION SYSTEM

The *Quarter of Vehicle (QoV)* model is often used when suspension modeling and control are considered. It allows to study the vertical behavior of a vehicle according to the suspension characteristics, Figure 1. This model offers a suitable representation of the problem to control the wheel load variations and forces in the suspension system.

The model shows the sprung mass (m_s), supported above the wheel and suspension assembly, referred to as the unsprung mass (m_{us}), which is supported by the tire, with a stiffness coefficient k_t, above the road surface. Between the sprung and unsprung masses are the *SA* damper with a force F_D and the suspension spring with a stiffness coefficient k_s.

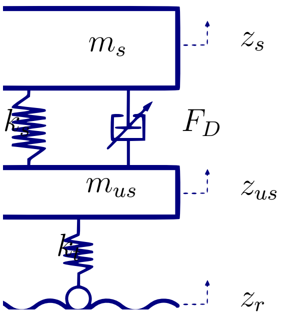

Fig. 1. Semi-Active Quarter of Vehicle model.

The dynamical equations that represent the *SA QoV* masses motion are:

$$\begin{cases} m_s \ddot{z_s} = -k_s(z_s - z_{us}) - F_D \\ m_{us}\ddot{z_{us}} = k_s(z_s - z_{us}) + F_D - k_t(z_{us} - z_r) \end{cases} \quad (1)$$

where F_D is the overall *SA* damping force from the *ER* damper, which is inherently nonlinear due to saturation, hysteresis, dynamic effect, etc. When no electric field is applied, the *ER* damper develops a damping force only produced by the fluid resistance. However, when a certain level of the electric field is applied, the *ER* damper generates an increased damping force due to the yield stress of the *ER* fluid. This damping force is able to be constantly adjusted by controlling the strength of the electric field. According to Guo et al. (2006), the damping force is:

$$F_D = k_0 \hat{z_{def}} + c_0 \dot{\hat{z}}_{def} + F_{ER} \quad (2)$$

where k_0 is the effective stiffness due to the gas pressure, c_0 is the effective damping due to the fluid viscosity, and F_{ER} is the controllable force which is a function of the applied electric field. The field dependent damping force F_{ER} is modeled as:

$$F_{ER} = f_c \tanh\left(a_1 \dot{\hat{z}}_{def} + a_2 \hat{z_{def}}\right) \cdot U \quad (3)$$

where the coefficients f_c, a_1 and a_2 are damper-dependent parameters, that vary according to each damper model; they can be exprimentally identified, and U is the control input, a *PWM* signal. To take the dynamic characteristic force, eqn (3) is expressed by:

$$\tau \frac{d}{dt} F_{ER} + F_{ER} = f_c \tanh\left(a_1 \dot{\hat{z}}_{def} + a_2 \hat{z_{def}}\right) \cdot U \quad (4)$$

$$F_{NL} = f_c \tanh\left(a_1 \dot{\hat{z}}_{def} + a_2 \hat{z_{def}}\right) \quad (5)$$

where τ stands for the time constant of damping force and F_{NL} contains the nonlinear behavior of the damper. By rearranging, the controlled damper force is:

$$\dot{F_{ER}} = -\frac{1}{\tau} F_{ER} + \frac{1}{\tau} F_{NL} \cdot U \quad (6)$$

These dynamic equations are shown in Figure 2; the damping force F_D is presented within the suspension system.

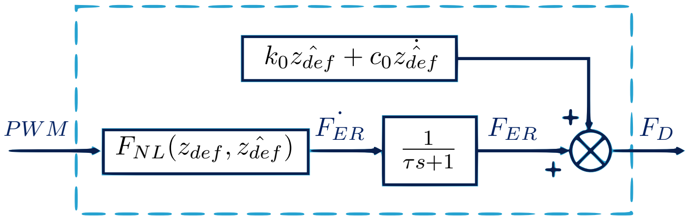

Fig. 2. *ER* dynamic model.

Remark. *The time constant τ depends on the ER fluid and might vary according to some factors (i.e. control input, fluid temperature, etc.); it is considered constant.*

3. OBSERVER DESIGN

The model used integrates the controllable damper force F_{ER} as a system state, the state-space model is given by:

$$\begin{cases} \dot{x}(t) = A\, x(t) + dB\, w_1(t) + B \cdot F_{NL}\, u(t) \\ y(t) = C\, x(t) + dC\, w_2(t) \end{cases} \quad (7)$$

where x is the state vector, w_1 the unknown road input, u the control input, y the measured variables, w_2 the measurements noise and $A \in \mathbb{R}^{n\times n}$, $dB \in \mathbb{R}^{n\times p}$, $B \in \mathbb{R}^{n\times p}$, $C \in \mathbb{R}^{q\times n}$, $dC \in \mathbb{R}^{q\times p}$ as follows:

$$x = [z_{def}\ \ \dot{z_s}\ \ t_{def}\ \ \dot{z_{us}}\ \ F_{ER}]^T \qquad y = [\ddot{z_s}\ \ \ddot{z_{us}}]^T$$

$$A = \begin{bmatrix} 0 & 1 & 0 & -1 & 0 \\ -\frac{(k_s+k_0)}{m_s} & -\frac{c_0}{m_s} & 0 & \frac{c_0}{m_s} & -\frac{1}{m_s} \\ 0 & 0 & 0 & 1 & 0 \\ \frac{(k_s+k_0)}{m_{us}} & \frac{c_0}{m_{us}} & -\frac{k_t}{m_{us}} & -\frac{c_0}{m_{us}} & \frac{1}{m_{us}} \\ 0 & 0 & 0 & 0 & -\frac{1}{\tau} \end{bmatrix}$$

$$dB = [0\ 0\ -1\ 0\ 0]^T \quad B = \left[0\ 0\ 0\ 0\ \tfrac{1}{\tau}\right]^T \quad dC = \begin{bmatrix} 0.1 \\ 0.005 \end{bmatrix}$$

$$C = \begin{bmatrix} -\frac{(k_s+k_0)}{m_s} & -\frac{c_0}{m_s} & 0 & \frac{c_0}{m_s} & -\frac{1}{m_s} \\ \frac{(k_s+k_0)}{m_{us}} & \frac{c_0}{m_{us}} & -\frac{k_t}{m_{us}} & -\frac{c_0}{m_{us}} & \frac{1}{m_{us}} \end{bmatrix}$$

3.1 H_∞ observer

Instead of estimating disturbances, the H_∞ observer offers a direct method to reduce the negative effect of disturbances in the states estimation.

The structure of the observer to estimate this model is:

$$\dot{\hat{x}}(t) = A\hat{x}(t) + L(y(t) - C\hat{x}(t)) + dB\ w_1(t) + BF_{NL} \cdot u(t)$$
$$\hat{x}_0 \text{ to be defined} \tag{8}$$

where $\hat{x} \in \mathbb{R}^{n\times n}$ is the estimated state of x and $L \in \mathbb{R}^{n\times n}$ is the observer matrix to be designed. The system (8) is said to be an H_∞ observer for the system (7) if:

$$\lim_{t\to\infty} e(t) \to 0 \text{ for } w(t) = 0$$
$$\left\| \frac{e(s)}{w(s)} \right\|_\infty = \|T_{ew}(s)\|_\infty \leq \gamma \text{ under } \hat{e}(t=0) = 0 \tag{9}$$

where $\|T_{ew}(s)\|_\infty$ is the H_∞ norm of the transfer function from the disturbances to the estimation error. The H_∞ estimation error dynamical equation, taking the unknown disturbances into account, can be expressed as:

$$\begin{aligned}\dot{e}(t) &= \dot{x}(t) - \dot{\hat{x}}(t)\\ &= (A - LC)e + (dB - LdC)w\end{aligned} \tag{10}$$

The estimated state variable $\hat{x}$, controlled by the error dynamics (10) converges asymptotically to the state x for any bounded initial conditions $\hat{x(0)}$ and $x(0)$ if and only if the following conditions are met, Darouach (2000).

Stability:

$$N = A - LC \tag{11}$$

where N is a Hurwitz or stable matrix.

Disturbance decoupling:

$$dB - LdC = 0 \tag{12}$$

The estimation error, described by (10), is driven by the unknown disturbance w. If an exact observer design, it is, where an exact disturbance decoupling is achieved since the estimated variables do not depend on the disturbance, is not possible, the disturbance effect on the estimated state variables can be minimized and is possible to compute an efficient observer. The method resides in applying the *Bounded Real Lemma (BRL)* to the error equation and apply a change of variables to obtain some *LMIs*.

Considering (7) and the observer (8). Given a positive scalar γ, if there exist $P = P^T \succ 0$ satisfying the inequality:

$$\begin{bmatrix} (A-LC)^T\mathbf{P} + \mathbf{P}(A-LC) & \mathbf{P}(dB - LdC) & I_n \\ \star & -\gamma I_d & O_{d,n} \\ \star & \star & -\gamma I_n \end{bmatrix} < 0 \tag{13}$$

then the observer (8) is an H_∞ observer according to 9.

The *BRL* applied to the error dynamics (10) gives the solution to (9) and leads to the *bilinear matrix inequality (BMI)* (13) where $\mathbf{P} = \mathbf{P}^T \succ 0$ and L are the unknown matrices to be determined. Thus, the full-order stable observer design problem consists in solving (13). It is possible to transform the *BMI* into a solvable *LMI* With a change of variables, let us define $\mathbf{Y} = -\mathbf{P}L$, leading to the following *LMI*:

$$\begin{bmatrix} A^T\mathbf{P} + \mathbf{P}A + \mathbf{Y}C + C^T\mathbf{Y}^T & \mathbf{P}dB + YdC & I_n \\ \star & -\gamma I_d & O_{d,n} \\ \star & \star & -\gamma I_n \end{bmatrix} < 0 \tag{14}$$

the observer gain will then be:

$$L = -\mathbf{P}^{-1}\mathbf{Y} \tag{15}$$

Finally, the proposed observer is synthesized so that the stability conditions in (11) are fulfilled, and the disturbance decoupling conditions in (12) are approximated by minimizing γ subject to (9).

3.2 Pole Placement

Stability is a minimum condition for control and estimation systems. However, in most real situations, a good observer should not only deliver an stability condition, but also to keep sufficiently fast and well-damped time responses. The preceding approach assures the observer stability and the disturbance effect minimization, but the observer poles are achieved through the solution of (13) and may be either very high, with high imaginary parts, or be almost unstable. A traditional approach to ensure suitable transients is to establish closed-loop poles in a convenient region of the complex plane, the idea is to make sure that the observer dynamics will be faster enough to accurately estimate the damper force in a real environment.

It is possible to use the quadratic Lyapunov function $V(z) = z^T P z$ to settle a lower bound on the decay rate of the system. If:

$$\frac{dV(x)}{dt} \leq -2\alpha V(x) \quad \textit{for all trajectories} \tag{16}$$

which is equivalent to

$$A^T P + PA + 2\alpha P \leq 0 \tag{17}$$

with this, it is possible to situate the observer poles within the region $\mathcal{D}_1$ in the complex plane, corresponding to a left half plane as represented in Fig. 3. This region is defined by the *LMI* (18), ensuring that the poles have real parts in $[-\infty, -\alpha]$.

$$\mathcal{D}_1 = z \in C : z + z^* + 2\alpha \prec 0 \tag{18}$$

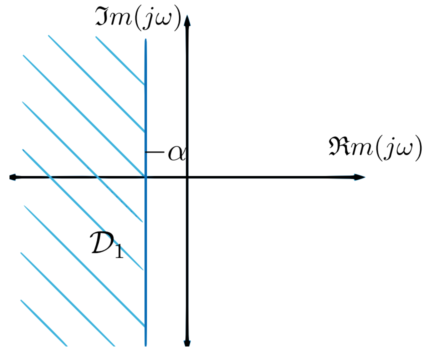

Fig. 3. LMI $\mathcal{D}_1$ region in the complex plane.

Then, from (14) and the pole placement approach the *LMI* to be solved is defined by:

$$\Phi = A^T\mathbf{P} + \mathbf{P}A + \mathbf{Y}C + C^T\mathbf{Y}^T + 2\alpha\mathbf{P}$$
$$\Psi = \mathbf{P}dB + YdC$$
$$\begin{bmatrix} \Phi & \Psi & I_n \\ \star & -\gamma I_d & O_{d,n} \\ \star & \star & -\gamma I_n \end{bmatrix} < 0 \tag{19}$$

where $\mathbf{P}$ and $\mathbf{Y}$ are the unknown matrices to be solved and α selected according to desired performance.

4. RESULTS

A QoV model of a 1:5 scale vehicle was used as test bench. An experimental model of a *ER* damper was considered. Both, simulation and experimental tests results are shown under different road conditions and control inputs. Table 1 shows the used model parameters.

Table 1. Model parameters

Parameter	Description	Value	Units
m_s	Sprung mass	2.27	kg
m_{us}	Unsprung mass	0.25	kg
k_s	Spring stiffness	1396	N/m
k_t	Tire stiffness	12270	N/m
k_0	Damper stiffness coefficient	186	N/m
c_0	Viscous damping coefficient	23	N·s/m
a_1	Velocity hysteresis coefficient	21	N·s/m
a_2	Disp. hysteresis coefficient	13	1/m
fc	Yield force of ER fluid	42	N
τ	Damper time constant	50	ms
U	*PWM* input	10	%

The road input is an unknown disturbance in the observer and both accelerations ($\ddot{z}_s$ and $\ddot{z_{us}}$) are used as the observer inputs. The evaluation of the *SA* damper force estimation system is composed in two steps:

(1) Assessment of the observer system for different tests in the time domain.
(2) Evaluation of the force estimation using a performance index.

4.1 Design of Experiments

The observer is tested under six different conditions in simulation and real tests with different road profiles and control inputs as follows:

(1) Bumps test with fixed 10% *PWM* input.
(2) Rough road with fixed 35% *PWM* input.
(3) *Chirp* road input with fixed 20% *PWM* input.
(4) Bumps test with variable *PWM* (Fig. 4 top).
(5) Rough road with variable *PWM* input (Fig. 4 top).
(6) *Chirp* road input with variable *PWM* (Fig. 4 bottom).

Two different *PWM* sequences are used according to the test, these inputs come from a uniformly distributed random signal between 0.05 and 0.40 and is saturated according to the control signal constraints $[0.10, 0.35]$, the first one is used in tests 4 and 5; while, the second one is used in the *Chirp* profile test, see Figure 4.

the implemented road profiles are shown in Fig. 5, the first one is a bumps test, then a rough road profile and finally a *Chirp* signal as a road input to test the observer under different frequencies.

To quantitatively evaluate the H_∞ observer performance, the *Error to Signal Ratio (ESR)* index was adopted. It is calculated as the ratio of the variance of the damper

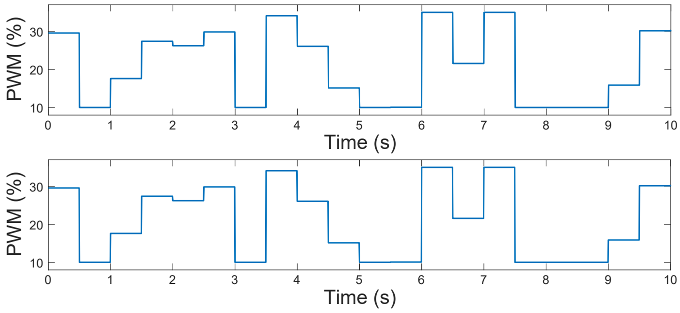

Fig. 4. *PWM* variations. Test 4 & 5 (top) and 6 (bottom).

force estimation error and the variance of the actual force, Savaresi et al. (2005):

$$ESR = \frac{Var(\hat{F_D} - F_D)}{Var(F_D)} \tag{20}$$

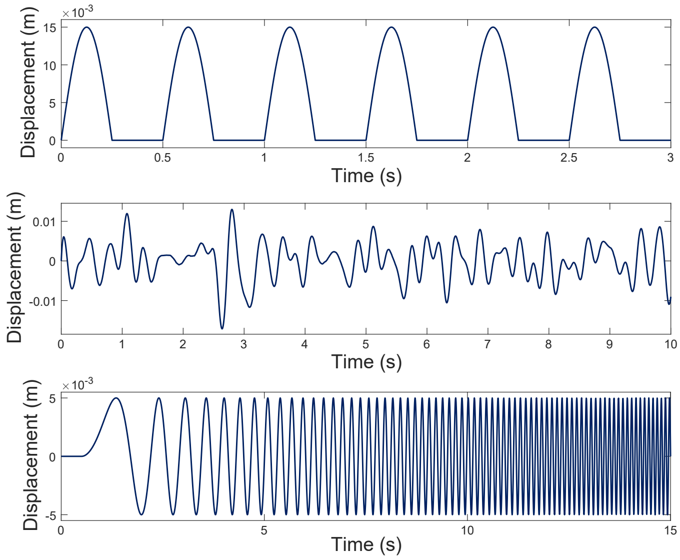

Fig. 5. Road profiles used for simulation tests. Road with bumps (top), Rough road (middle), Chirp (bottom)

The adoption of this time domain performance index allows to deal with the nonlinear effects of the *ER* damper, which are more difficult to consider when using traditional *Root Mean Square Error (RMSE)* analysis. It is important to note that the *ESR* remains in the range $[0, 1]$, where a value of 0 expresses a perfect estimation, while a value of 1 points out that the observer is only able to predict the mean value of the damper force.

Additionally to the *ESR* performance index, the *Normalized Root-Mean-Square Error (NRMSE)* was computed for each test to compare the estimation in terms of percentage. This index is a way of measuring how good our estimated model is over the actual data and is sensitive to outliers. It computes the square root of the *Mean Squared Error (MSE)* and then normalizes it by dividing by the force estimation range:

$$NRMSE = \frac{\sqrt{MSE(\hat{F_D}, F_D)}}{max(\hat{F_D}) - min(\hat{F_D})} \tag{21}$$

4.2 Simulation

Each of the six conditions listed before are tested in simulation, tests were done with initial values in the observer different than zero, to evaluate the transient state behavior in the initial stage. A qualitative analysis can be made by plotting simulations results. Aiming to show the observer trackability, only results in damper force estimation of test 2 and 4 are shown in Figs. 6-7.

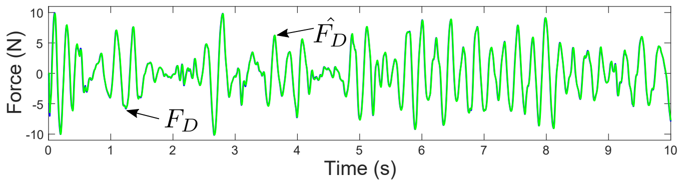

Fig. 6. Damper force simulation in test 2.

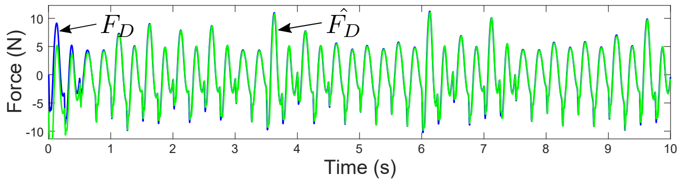

Fig. 7. Damper force simulation in test 4.

4.3 Experiments

The performance of the H_∞ observer has been investigated with numerical simulations and the proposed observer seems to be effective. Some experimental tests in the real test bench are presented.

The experimental platform consists in a 1:5 scale vehicle that has been developed as part of the *INOVE* [1] project. The test bench has been designed to analyze the vehicle vertical behavior with sensors placed to measure some variables, which describe the vehicle dynamics.

The road profile is simulated using 4 linear motors applying vertical displacements to each wheel. Only the front right corner, which consists in a double-wishbone suspension, has been used to test the developed damper force observer. The measured variables are shown in Fig. 8 according to: (1) *ER* Damper force (F_D), (2) Sprung mass acceleration ($\ddot{z_s}$), and (3) Unsprung mass acceleration ($\ddot{z_{us}}$).

Fig. 8. *INOVE* test-bench and sensors.

[1] Integrated approach for observation and control of vehicle dynamics, http://www.gipsa-lab.fr/projet/inove/

Additionally, four *SA* suspensions of *SOBEN* [2] have been mounted thus replacing the original passive suspension. The suspension system comprises four *ER* dampers, which have a force range of ±30 N. These dampers are regulated using a manipulation voltage between 0 and 5 kV, which is generated by the amplifiers modules. The control input for the modules is a PWM signal at 25 kHz. These amplifiers proportionally transform the duty-cycle of the received PWM signal into a voltage.

The decay rate α, which is an observer design parameter, has been set to $\alpha = 10$, this value showed the best performance based on experimental tests.

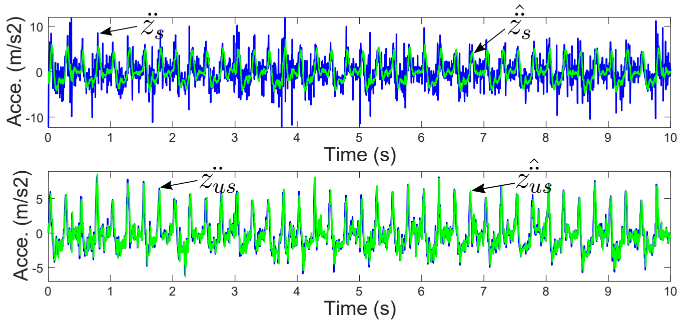

Fig. 9. Sprung and unsprung mass accelerations in test 1.

As well as in simulation, a qualitative analysis was done by plotting simulations results in the time domain. For the sake of brevity, and aiming to show the observer trackability, only the accelerations for the first test are shown in Fig. 9, where is clear that the observer follows the acceleration measurements filtering the high noise signals. For the remaining tests only damper force estimation results are shown in Figures 10 and 11.

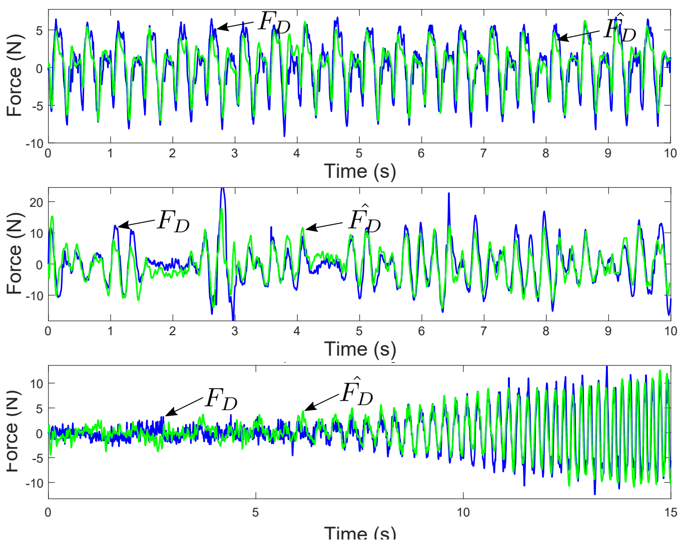

Fig. 10. Damper force in test 1 (top), test 2 (middle) and test 3 (bottom).

From tests 1 and 2, it is fair to say that the observer follows the damper force behavior, although, in some parts the estimation seems a little bit underestimated. The test 3 shows the *Chirp* road profile, the estimation is good in

[2] *SOBEN* is a specialized company in innovative shock absorbers, http://www.soben.fr/

general, despite the fact that estimation does not seems good in low frequency, this is mainly due the high noise in the sensors and low relative motion in the initial stage.

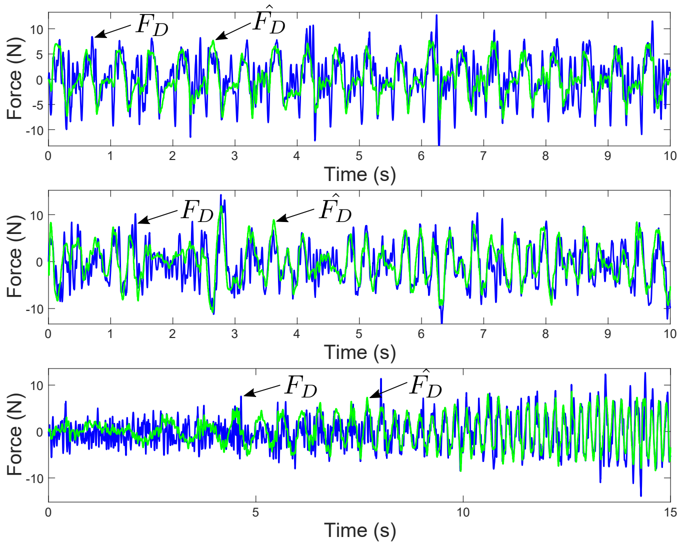

Fig. 11. Damper force in test 4 (top), test 5 (middle) and test 6 (bottom).

4.4 Discussions

A quantitative analysis is shown in Table 2. The *ESR* and *NRMSE* values for each test shows that the observer is able to track accurately the actual damper force under different road and control input conditions in simulation and real experiments. In the case of simulation tests the table was computed without taking the initial transient phase of the observer into account. There is a deterioration in the damper force estimation when a variable control input is applied in comparison with the fixed *PWM*.

Table 2. *ESR* and *NRMSE* results for real tests

Test	***ESR***		***NRMSE***	
	Simulation	**Real**	**Simulation**	**Real**
1	0.0622	0.2298	2.48 %	11.52 %
2	0.0104	0.3356	1.86 %	8.25 %
3	0.0386	0.2875	1.64 %	8.18 %
4	0.0622	0.5909	1.99 %	12.03 %
5	0.0169	0.5387	1.87 %	11.32 %
6	0.0480	0.6086	1.63 %	10.29 %

It is clear that the simulation results are far more accurately, in the case of *ESR* values real data shows, in average, an error 10 times higher while with the *NRMSE* index, the values in real tests are around five times higher. When implementing this estimated force in a *FCS*, the controller should be robust enough to handle this estimation error.

Not much work has been done in *SA* damper force estimation, Eroglu and Sims (2014) developed an observer based controller, where the damper force estimation is used for control purposes in a *SDOF* system; nonetheless, the observer requires the disturbance to estimate the force, which would be a costly solution for real applications, and the model does not take the damper dynamics into account, the current work was developed looking to tackle this limitations, considering an unknown road input and the damper dynamics.

5. CONCLUSIONS

An H_∞ observer for the *SA* damper force estimation of an *ER* damper in a vehicle suspension under an unknown road disturbance has been proposed. The *ER* damper model dynamics has been integrated in the *QoV* model dynamics and have been structured into a single five states system, handling the non-linearities and dynamic behavior in the damper. Several *SA* suspension control systems compute the desired damper force rather than the physical control signal for the damper; thus, a control loop is needed to transform the desired force to the damper manipulation signal or an inverse model dynamics of the *ER* damper is required, which could harm the system controllability due to the *ER* hysterical behavior.

The observer solves the complexity of the *FCS* based on feedback linearization theory with acceleration measurements. The design of robust observer within the H_∞ framework plays a key role in the performance of the proposed estimation method. The developed methodology includes both the performance specifications and measurement noise filtering. *SA* suspension control is a very challenging problem in the automotive industry and within the automation research community as well, where the reduced number of sensors and cost implementation are a key point in the design process.

REFERENCES

Batterbee, D.C. and Sims, N.D. (2007). Hardware-in-the-Loop Simulation of Magnetorheological Dampers for Vehicle Suspension Systems. *J. of Systems and Control Eng*, 221(2), 265–278.

Besinger, F., Cebon, D., and Cole, D. (1995). Force Control of a Semi-Active Damper. *Vehicle System Dynamics*, 24(April), 695–723.

Darouach, M. (2000). Existence and Design of Functional Observers for Linear Systems. *IEEE Trans. on Automatic Control*, 45(5), 940–943.

Dugard, L., Sename, O., Aubouet, S., and Talon, B. (2012). Full Vertical Car Observer Design Methodology for Suspension Control Applications. *Control Eng. Practice*, 20(9), 832–845.

Eroglu, M.A. and Sims, N.D. (2014). Observer Based Optimal Control of MR Dampers. In *Proc. of the* 10^{th} *World Congress on Computational Mechanics*, volume 1, 5040–5051. Blucher, São Paulo.

Guo, S., Yang, S., and Pan, C. (2006). Dynamic Modeling of Magnetorheological Damper Behaviors. *J. of Intell. Mater., Syst. and Struct.*, 17(1), 3–14.

Savaresi, S.M., Bittanti, S., and Montiglio, M. (2005). Identification of Semi-Physical and Black-Box Non-Linear Models: The case of MR-Dampers for Vehicles Control. *Automatica*, 41(1), 113–127.

Sims, N.D., Stanway, R., and Beck, S.B.M. (1997). Proportional Feedback Control of an Electro-Rheological Vibration Damper. *J. of Intelligent Material Systems and Structures*, 8(May), 426–433.

Vivas-Lopez, C., Hernandez-Alcantara, D., Nguyen, M.Q., Morales-Menendez, R., and Sename, O. (2015). Force Control System for an Automotive Semi-Active Suspension. *IFAC-PapersOnLine*, 48(26).